THE JOURNAL OF PHYSICAL CHEMISTRY Letters

Letter

pubs.acs.org/JPCL

Nano Pinstripes: TiO_2 Nanostripe Formation by Nanoparticle-Mediated Pinning of Step Edges

F. Behafarid and B. Roldan Cuenya*

Department of Physics, University of Central Florida, Orlando, Florida 32816, United States

ABSTRACT: The present scanning tunneling microscopy study describes the high-temperature growth of TiO_2 nanostripes with tunable width, orientation, and spacing, mediated by thermally stable micellar Pt and Au NPs deposited on $TiO_2(110)$. This phenomenon could not be explained by spillover effects but is based on the preferential stabilization of $[1\bar{1}0]$ step edges on $TiO_2(110)$ by the metal NPs. Contrary to the behavior of physical-vapor-deposited NPs, which are known to move toward step edges upon annealing, our micellar NPs remain immobile up to 1000 °C. Instead, the mobility of TiO_2 step edges toward the micellar NPs, where they become stabilized, is observed. Our findings are relevant to the technological application of nanostructured materials in the fields of catalysis, molecular electronics, and plasmonics.

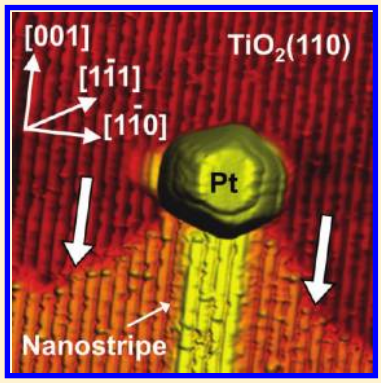

SECTION: Nanoparticles and Nanostructures

The unusual structural, electronic, magnetic, and chemical properties of metallic nanostructures have been proven to be useful for numerous applications in technologically important areas such as catalysis, molecular electronics, nanomedicine, energy conversion, and plasmonics.[1−6] Nevertheless, to take advantage of these new material systems in an industrial setting, a thorough understanding of how those properties are affected by their environment (support and surrounding adsorbates) as well as operation condition (e.g., elevated temperature) is needed. The present study provides insight into the interaction of micellar metal NPs with oxide supports. There are numerous studies showing how different supports could affect the shape, electronic structure, catalytic properties, and coarsening behavior of nanoparticles (NPs).[7−11] However, less is known about the changes brought about by the presence of the NPs on the support itself, including its reconstruction and patterning. Here we demonstrate that micellar Au and Pt NPs can serve as nucleation centers for the growth of [001]-oriented TiO_2 nanostripes on the surface of $TiO_2(110)$ upon annealing in ultrahigh vacuum (UHV) at and above 1000 °C. Such surfaces are expected to display a modified reactivity because [001] step edges have been recently shown to give rise to higher photocatalytic activity for certain photodegradation reactions as compared with $[1\bar{1}1]$ step edges.[12] Therefore, surface engineering methods that provide the ability to tune the density of certain step edges are desirable. The realization of this idea in an easily scalable manner is presented here.

Figure 1 displays STM images of TiO_2-supported micellar NPs in (a,c−f) S1 and (b) S2 acquired after annealing in UHV above 1000 °C. The average size of the Pt NPs in S1 is ∼3.0 nm, and their average interparticle distance is ∼30 nm, and both parameters remained nearly constant after annealing in UHV from 1000 to 1060 °C (Figure 1a.) The enhanced thermal stability of micellar Pt NPs as compared with physical vapor deposited (PVD) clusters might be assigned to the following factors: (i) Coarsening phenomena based on diffusion-coalescence processes might be minimized for the micelle-based samples due to their large and homogeneous interparticle distances and relatively low NP density on the support. (ii) The narrower initial NP size distribution in the micellar samples might inhibit Ostwald-ripening pathways in which large clusters grow at the expense of smaller NPs. (iii) The micellar NPs are exposed to atomic oxygen at room temperature prior to the thermal treatment, which leads to NP oxidation. Even though the PtO_x species formed are expected to be decomposed at the high annealing temperatures employed here,[14,15] the former treatment might contribute to strengthening the initial binding between the Pt NPs and the TiO_2 support, leading to their subsequent stabilization. Although our Pt NPs are mostly oxidized after the initial O_2-plasma treatment used for the removal of organic ligands from the NP surface, XPS measurements have shown their reduction after annealing in UHV at temperatures above 450 °C.[14,15] Nevertheless, because of the low NP coverage in our samples and the limitations in the sensitivity of XPS, we cannot rule out the presence of PtO_x at the NP/support interface. Such species might influence the coarsening behavior of the micellar NPs. Further details of the stability of the $Pt/TiO_2(110)$ system are reported in our previous work.[13] In addition, the present high-temperature annealing treatments results in surface/bulk melting of our NPs, as evidenced by the faceted shapes and

Received: January 6, 2012
Accepted: February 10, 2012
Published: February 10, 2012

   dx.doi.org/10.1021/jz300022c | J. Phys. Chem. Lett. 2012, 3, 608−612

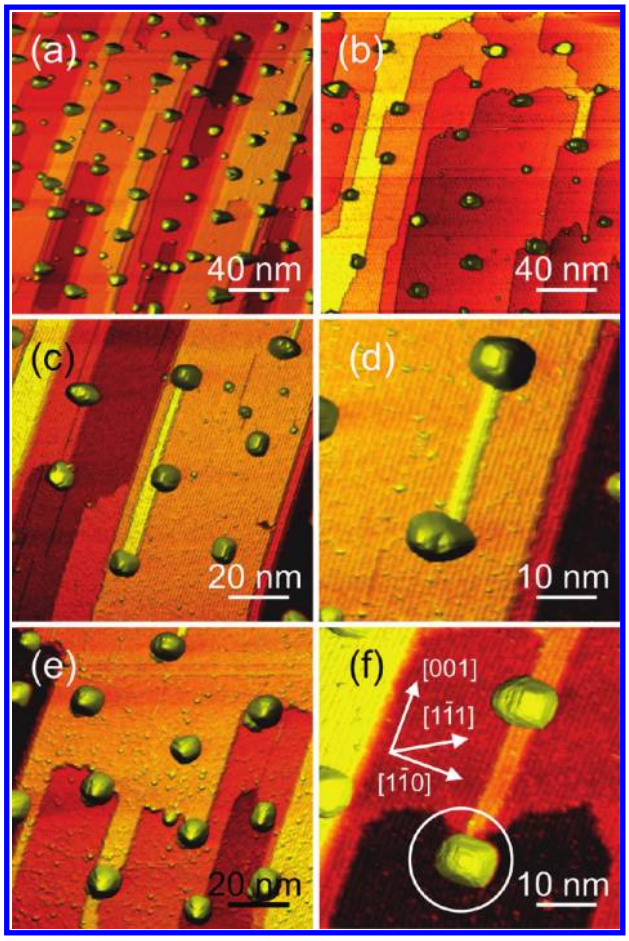

Figure 1. Room -temperature STM images of micellar Pt NPs in samples S1(a,c–f) and S2 (b), deposited on TiO_2 (110) and acquired after polymer removal by an in situ O_2-plasma treatment and subsequent isochronal annealing in UHV at 1010 (a,b), 1020 (c,d), and 1060 °C (e,f).

epitaxial NP/TiO_2 relationship adopted by the NPs upon cooling (Figure 2b and ref 16).

Because the polymer used in the synthesis of S2 had longer head and tail lengths, the resulting Pt NPs were characterized by larger average sizes (~3.7 nm) and larger average interparticle distances (~40 nm) (Figure 1b). Interestingly, the STM images in Figures 1 and 2 reveal the formation of TiO_2 nanostripes on the Pt NP-coated TiO_2(110) surface upon annealing. This is in striking contrast with the behavior observed on NP-free TiO_2 surfaces[13,17] or those decorated by PVD-grown NPs after annealing at room temperature,[18] 400–730 °C,[9,19] or similar conditions to our experiment (1000–1060 °C).[20] Our TiO_2 nanostripes were found to be attached to the NPs and have a preferential growth direction along the [001] orientation of the TiO_2(110) substrate. The width of these nanostripes was found to be similar to the NP diameter (3–5 nm), and their length was found to be as large as 80 nm. Interestingly, at the highest annealing temperatures employed (1040 and 1060 °C), the TiO_2 nanostripes start to become detached from the Pt NPs (see white circle in Figure 1f). Further annealing lead to the growth of wider TiO_2 terraces in detriment of the narrow TiO_2 nanostripes.

The Pt/TiO_2 system is characterized by strong metal–support interactions (SMSI).[21−24] This includes support-induced changes in the electronic properties of the Pt NPs

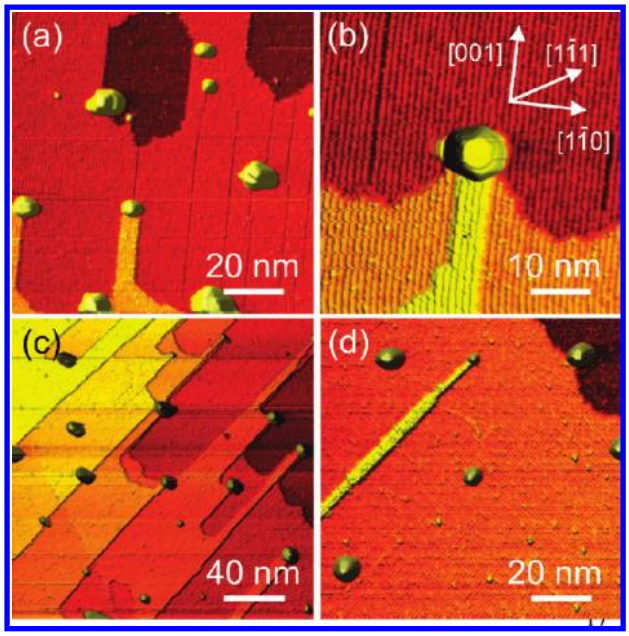

Figure 2. Room-temperature STM images of Pt NPs in S2 (a,b) and Au NPs in S3 (c,d) on TiO_2(110) acquired after annealing in UHV at 1000 °C for 10 min.

and Pt encapsulation by ultrathin TiO_x layers. Therefore, the formation of the TiO_2 nanostripes observed here for the Pt/TiO_2 system could be intuitively attributed to some degree of SMSI effect. However, this possibility is disregarded because identical trends were observed for Au/TiO_2, a system that does not show the SMSI effect (Figure 2c,d). The main difference between our micellar Au and Pt NPs on TiO_2(110) is the fact that because of the lower melting temperature of Au, the initial hexagonal NP arrangement[13,16] is lost for the Au NPs after annealing at elevated temperatures (>1000 °C, Figure 2c,d), and thus the spacing between the TiO_2 nanostripes formed is not uniform, as is the case for Pt/TiO_2.

Different mechanisms have been reported in the past as being responsible for the reconstruction of NP-decorated oxide surfaces. For example, by annealing in oxygen environments, TiO_2 islands were found to grow around PVD Pt and Pd NPs on TiO_2(110).[25,26] In the former examples, oxygen was found to dissociate on the NP surface and spillover from the NPs to the support, resulting in the segregation of Ti interstitials from the bulk to the surface of the TiO_2 crystal and the formation of TiO_x islands around the NPs. Nevertheless, nanostripes such as those shown in Figures 1 and 2 were never obtained, and the former effects were observed upon annealing at lower temperatures (<500 °C) and in the presence of oxygen. In fact, even in oxygen environments, higher annealing temperatures (>550 °C), such as those employed in our experiments, were reported to inhibit this effect.[27] Vapor–liquid–solid growth processes[28,29] mediated by the metal NPs can also not be held responsible for the growth of the TiO_2 nanostripes observed here because such growth requires the presence of titanium vapor, which was not available in our experiments. Preferential diffusion of TiO_x species activated by the metal NPs[30] cannot explain the formation of our nanostripes because such phenomenon should have led to the formation of stripes on both sides of the NPs, which is not observed here.

Before discussing the actual growth mechanism of our nanostripes, we would like to point out the distinct properties

dx.doi.org/10.1021/jz300022c | J. Phys. Chem. Lett. 2012, 3, 608–612

of our micellar NPs as compared with more conventionally synthesized NPs. Whereas mobile PVD NPs are known to preferentially decorate at vacancies and TiO_2 step edges,[9,13,18−20] the same does not apply to the micellar NPs. This is due to the fact that the micellar NPs are surrounded by polymeric ligands upon initial deposition on the TiO_2 surface and that the TiO_2 surface is roughened during the ex situ (air) NP deposition.[16] Nevertheless, as can be seen in Figures 1 and 2 and ref 13, a large fraction of the micellar NPs was located at step edges after high-temperature annealing treatments. Because we have shown that the micellar Pt NPs are resistant against diffusion even after extreme thermal treatments (>1000 °C)[13,16] and because their quasi-hexagonal arrangement is still preserved (see Figure 1a−c,e), it can be concluded that rather than the NPs moving toward the step edges of TiO_2, the step edges moved toward the NPs. To understand this phenomenon, we should consider the diffusion of Ti and O species in TiO_2 and the effect of the bulk and surface stoichiometry of our single-crystal oxide support. It has been shown that the bulk reduction state of TiO_2 plays an important role in the resulting surface reconstruction.[31] After numerous cycles of Ar^+ sputtering and annealing (900−1000 °C) in vacuum, the degree of reduction of our TiO_2 single crystal was very high, as evidenced by its dark blue color and (1 × 2) surface reconstruction before NP deposition.[17,27,32] The subsequent dip-coating of the micellar NPs in air followed by the in situ O_2-plasma treatment (polymer removal) results in the oxidation of the TiO_2 surface. Nevertheless, the succeeding annealing treatments in UHV at high temperature (>900 °C) are expected to lead to the desorption of surface oxygen, whereas Ti cations (Ti^{3+}) diffuse inward from the surface to the bulk of the crystal.[27,32,33] At this point, significant changes in the morphology of our TiO_2 surface were found to occur, in particular, the formation of TiO_2 nanostripes.

Two key aspects of our experimental observation should be considered to understand the NP-mediated growth mechanism of the TiO_2 nanostripes. First, in most cases the stripes are attached to only one side of the NPs, while conventional TiO_2 growth/reconstruction mechanisms such as those based in spillover effects result in islands surrounding the NPs.[27,34] Second, if the TiO_2 nanostripe growth would result from the diffusion of Ti adatoms on the TiO_2(110) surface, then the extremely large aspect ratio of the nanostripes observed here would require a very large diffusion anisotropy constant. As previously mentioned, the width of our nanostripes follows very closely the diameter of the NPs; their length reaches several tens of nanometers in the [001]direction, but there is almost no nanostripe growth along [1$\bar{1}$0]. Because of tip-convolution effects inherent to all scanning probe microscopy techniques, an exact evaluation of the NPs' lateral dimensions is not feasible, especially for small NPs with 3D shape.[16] Therefore, a quantitative claim regarding the correlation between the diameter of our NPs and the width of the stabilized TiO_2 nanostripes cannot be made. However, the majority of our images suggest that the nanostripe width is either equal to or smaller than the diameter of the NPs attached to them.

The former trends would suggest a 1-D diffusion phenomenon along [001]. Nevertheless, previous ab initio calculations[35] and also experimental results[36] do not support this hypothesis. In fact, because of the existence of different diffusion mechanisms, the barrier for Ti diffusion was found to be lower along [1$\bar{1}$0] than in the [001]direction.[35] In addition, it was shown that interstitial Ti atoms are more energetically favorable than adatoms on the surface[37] and that the energy barrier to go subsurface should be easily overcome during our high-temperature annealing treatments. Therefore, any Ti adatoms that might be present on our surface would not have a tendency to diffuse on the surface but instead would go subsurface.

The above arguments justify our conclusion that neither spillover effects nor preferential diffusion of Ti adatoms on the TiO_2 surface is responsible for the nanostripe growth observed here. Instead, we propose a mechanism based on diffusion/mass transfer perpendicular to the surface, also involving the stabilization of certain TiO_2 step edges by the micellar NPs. Previous high-temperature (~730 °C) STM snapshots of pristine TiO_2(110) had shown the loss of material upon annealing in vacuum, evidenced by the observation of receding step edges.[27,32] In the previous studies, the gradual disappearance of the topmost TiO_2 terraces was assigned to the desorption of oxygen to vacuum and the migration of the titanium that is left behind into the bulk.[27,32] Interestingly, this gradual disappearance of TiO_2 rows starts at [1$\bar{1}$0] step edges and follows a chain reaction that proceeds along TiO_2 rows in the [001] direction.[27] This phenomenon, illustrated in Figure 3,

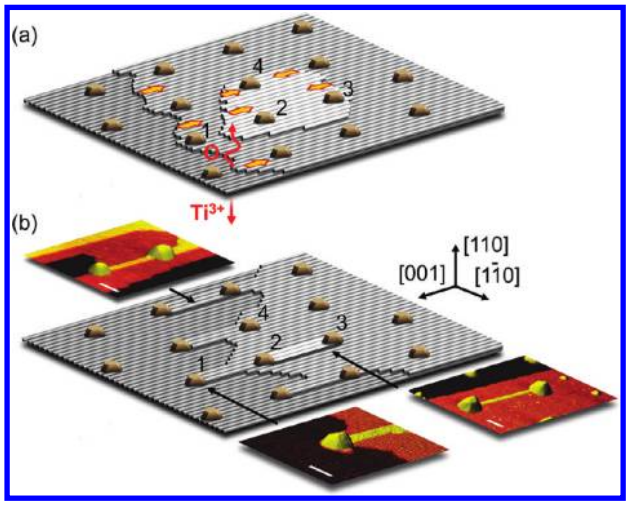

Figure 3. Schematics showing the formation of nanostripes attached to micellar NPs. Upon sample annealing above 1000 °C in UHV, oxygen (O) desorbs from the TiO_2(110) surface to vacuum and Ti^{3+} goes into the bulk of the crystal. TiO_2 rows along the [001]direction shrink in length and in some cases disappear. However, the stabilization of [1$\bar{1}$0] TiO_2 step edges by micellar NPs prevents the disruption of the rows attached to the NPs, resulting in the formation of nanostripes. The insets in panel b correspond to STM images representative of this process. The white scale bars in the STM images correspond to 10 nm.

is the most likely mechanism behind the nanostripe formation observed in our study. Pt or Au micellar NPs stabilize low-coordinated atoms at TiO_2 [1$\bar{1}$0] step edges and therefore prevent the disintegration of the TiO_2 structure that is in contact with the NPs along [1$\bar{1}$0] steps. Whereas the majority of the topmost TiO_2 [1$\bar{1}$0] step edges retreat (see arrows in Figure 3a), those attached to NPs remain stable because of the passivation of the oxygen desorption sites. The remaining stable TiO_2 rows give rise to TiO_2 nanostripes with a width similar to the diameter of the NPs. Interestingly, this is also in agreement with the observation that most of the nanostripes are attached just to one side of the NPs, in contrast with spillover mechanisms that should have resulted in growth on both sides.

dx.doi.org/10.1021/jz300022c | J. Phys. Chem. Lett. 2012, 3, 608−612

A few different nanostripe formation possibilities, based on the relative locations of the NPs on the TiO_2 surface, are highlighted in Figure 3b. The TiO_2 terrace underneath the NP labeled as 1 has no step edge on its right-hand side; therefore, the desorption of oxygen happens only on the left side through the $[1\bar{1}0]$ step edge. This results in the formation of a nanostripe on the right side of the NP. In some cases, a few TiO_2 rows are protected at both ends by NPs, as it is shown between NPs 2 and 3 in Figure 3b. Also, the terraces with $[1\bar{1}0]$ step edges on both sides of a NP may disappear completely and not result in nanostripe formation because both step edges would move toward the NP and vanish entirely, as the terraces around NP4 in Figure 3b. This mechanism could also explain the large aspect ratio of the nanostripes. In this scenario, the length of the nanostripes is not limited by diffusion anisotropy and only depends on the configuration of the TiO_2 terraces in the vicinity of the NPs.

A similar in situ atomic oxygen treatment, followed by high-temperature heating in UHV recently conducted on small PVD-grown Pt NPs (~1.3 nm), did not result in the nanostripe formation demonstrated here.[20] A possible explanation might be size-dependent cluster mobility. The smaller PVD clusters may be partially stabilized by step edges, reducing their mobility along certain substrate orientations, whereas at the high annealing temperatures required for the TiO_2 reconstruction and nanostripe formation (>900 °C) PVD, cluster mobility along the step edges might still occur. This would limit the step-edge pinning needed for nanostripe formation. For the larger (~3 nm) micellar NPs, the particle mobility is expected to be reduced, enabling step-edge pinning at high temperature. This interpretation is supported by the fact that the NP diffusion coefficient is inversely proportional to its radius ($D \approx 1/r^4$), making the larger micellar particles significantly less mobile.[9,20] Additionally, intrinsic differences in the shape of the micellar[16] (mainly 3D-like) and PVD NPs (mainly 2D-like) after our in situ treatments might also influence their ability to stabilize certain steps edges. Because our preliminary data on PVD-grown NPs targeted smaller NP sizes as compared with the typical average micellar NP size investigated here, it cannot be ruled out that analogously pretreated but larger PVD NPs might also produce nanostripe patterns.

Even though TiO_2 step edges are known to stabilize metal NPs, we have shown that the opposite trend also occurs; namely, immobile NPs can stabilize step edges. The enhanced thermal stability of micellar NPs against coarsening and diffusion has allowed us to observe the changes in the underlying support surface around the micellar NPs. In contrast with metal surfaces in which the surface reconfiguration/reconstruction occurs mainly through surface diffusion of adatoms,[38] the present example illustrates the diffusion of Ti cations perpendicular to the surface into the bulk of $TiO_2(110)$ upon oxygen desorption at elevated annealing temperatures. The former effect is responsible for the drastic morphological changes observed on our $TiO_2(110)$ surface, in particular, for the formation of TiO_2 nanostripes along [001] stabilized by the micellar NPs. It should also be noted that our TiO_2 nanostripes are highly reduced because they display a (1×2) reconstruction typical of reduced TiO_2 surfaces. Because oxygen desorption occurs at the TiO_2 surface, a lower degree of reduction is expected for the bulk of the TiO_2 substrate. Although a quantification of the subsurface conductivity cannot be carried out based on the experimental tools at hand, a higher electrical conductivity is expected for the TiO_2 layers closer to the surface as well as for the nanostripes.[39] Because our synthesis method can lead to NPs interconnected by reduced TiO_2 nanostripes (Figures 1c,d and 3), they might hold promise as self-organized NP contacts on higher bandgap TiO_2 substrates. Finally, our findings open the possibility of using metallic micellar NPs to pattern oxide surfaces, generating uniform arrays of oxide nanostripes with tunable width (related to NP diameter), orientation, and interwire distance (related to interparticle distance).

EXPERIMENTAL SECTION

Size-selected Pt and Au NPs were prepared by a reverse micelle encapsulation method[13,14,40−42] using two commercial diblock copolymers, polystyrene-*block*-poly(2-vinylpyridine) [P1: PS(27700)-PVP(4300) and P2: PS(81000)-P2VP(14200)]. Metal salts, $HAuCl_4 \cdot 3H_2O$ and $H_2PtCl_6 \cdot 6H_2O$, were added to separate polymeric solutions previously obtained by dissolving 50 mg of the PS-P2VP in 10 mL of toluene. Using this synthesis method, the NP size as well as their interparticle distance can be controlled independently.[13,14,40−42] The length of the diblock-copolymer core (P2VP) and the metal-salt/P2VP concentration ratio determines the NP size, whereas the interparticle distance can be tuned by modifying the length of the PS tail. In the present case, P2 is expected to result in NPs spaced by larger distances as compared with P1, as seen in Figure 1a,b. We prepared three different samples: samples S1 and S2 contain Pt NPs and were synthesized using polymers P1 and P2, respectively, whereas S3 included Au NPs encapsulated by P2. The metal loadings (metal/P2VP ratio) used were 0.6 for S1 and 0.3 for S2 and S3. A self-assembled monolayer of NPs on the $TiO_2(110)$ substrate was obtained by dip-coating the single crystal into the Au or Pt polymeric solutions at a speed of 200 μm/s.

Upon ex situ NP deposition, the removal of the encapsulating polymer was carried out in UHV by an oxygen-plasma treatment (O_2 pressure = 4×10^{-5} mbar, 90−120 min). No residual C signal was detected by X-ray photoelectron spectroscopy (XPS) after this treatment,[13,14,40−42] but the NP surface became oxidized. Subsequently, the micellar samples were isochronally annealed in UHV in 100 °C intervals from 300 to 800 °C for 20 min, a treatment that stabilized the NPs against coarsening, followed by isochronal annealing at and above 900 °C for 10 min and in 10 °C increments from 1000 to 1060 °C. Scanning tunneling microscopy (STM) images were measured at room temperature (Aarhus-STM, SPECS GmbH) after several of the annealing treatments. The tunneling voltage was set to 1.2 V, and the tunneling current was set to 0.1 nA.

AUTHOR INFORMATION

Corresponding Author

*E-mail: roldan@ucf.edu.

Notes

The authors declare no competing financial interest.

ACKNOWLEDGMENTS

Financial support from the Office of Basic Energy Science of the U.S. Department of Energy (DE-FG02-08ER15995) is greatly appreciated.

REFERENCES

(1) Bell, A. T. The Impact of Nanoscience on Heterogeneous Catalysis. *Science* **2003**, *299*, 1688−1691.

(2) Jain, P. K.; Huang, X.; El-Sayed, I. H.; El-Sayed, M. A. Review of Some Interesting Surface Plasmon Resonance-enhanced Properties of Noble Metal Nanoparticles and Their Applications to Biosystems. *Plasmonics* **2007**, *2*, 107−118.
(3) Somorjai, G. A.; Frei, H.; Park, J. Y. Advancing the Frontiers in Nanocatalysis, Biointerfaces, and Renewable Energy Conversion by Innovations of Surface Techniques. *J. Am. Chem. Soc.* **2009**, *131*, 16589−16605.
(4) Shiju, N. R.; Guliants, V. V. Recent Developments in Catalysis Using Nanostructured Materials. *Appl. Catal., A* **2009**, *356*, 1−17.
(5) Raffa, V.; Vittorio, O.; Riggio, C.; Cuschieri, A. Progress in Nanotechnology for Healthcare. *Minim. Invasive Ther.* **2010**, *19*, 127−135.
(6) Christopher, P.; Xin, H.; Linic, S. Visible-Light-Enhanced Catalytic Oxidation Reactions on Plasmonic Silver Nanostructures. *Nat. Chem.* **2011**, *3*, 467−472.
(7) Henry, C. R. Surface Studies of Supported Model Catalysts. *Surf. Sci. Rep.* **1998**, *31*, 235−325.
(8) Roldan Cuenya, B. Synthesis and Catalytic Properties of Metal Nanoparticles: Size, Shape, Support, Composition, And Oxidation State Effects. *Thin Solid Films* **2010**, *518*, 3127−3150.
(9) Jak, M. J. J.; Konstapel, C.; van Kreuningen, A.; Chrost, J.; Verhoeven, J.; Frenken, J. W. M. The Influence of Substrate Defects on the Growth Rate of Palladium Nanoparticles on a TiO_2(110) Surface. *Surf. Sci.* **2001**, *474*, 28−36.
(10) Guo, Q. L.; Luo, K.; Davis, K. A.; Goodman, D. W. Initial Growth of Au on Oxides. *Surf. Interface Anal.* **2001**, *32*, 161−165.
(11) Campbell, C. T. Ultrathin Metal Films and Particles on Oxide Surfaces: Structural, Electronic and Chemisorptive Properties. *Surf. Sci. Rep.* **1997**, *27*, 1−111.
(12) Takahashi, H.; Watanabe, R.; Miyauchi, Y.; Mizutani, G. Discovery of Deep and Shallow Trap States from Step Structures of Rutile TiO_2 Vicinal Surfaces by Second Harmonic and Sum Frequency Generation Spectroscopy. *J. Chem. Phys.* **2011**, *134*, 154704.
(13) Naitabdi, A.; Behafarid, F.; Roldan Cuenya, B. Enhanced Thermal Stability and Nanoparticle-Mediated Surface Patterning: Pt/TiO_2(110). *Appl. Phys. Lett.* **2009**, *94*.
(14) Ono, L. K.; Yuan, B.; Heinrich, H.; Roldan Cuenya, B. Formation and Thermal Stability of Platinum Oxides on Size-Selected Platinum Nanoparticles: Support Effects. *J. Phys. Chem. C* **2010**, *114*, 22119−22133.
(15) Ono, L. K.; Croy, J. R.; Heinrich, H.; Cuenya, B. R. Oxygen Chemisorption, Formation, and Thermal Stability of Pt Oxides on Pt Nanoparticles Supported on SiO_2/Si(001): Size Effects. *J. Phys. Chem. C* **2011**, *115*, 16856−16866.
(16) Behafarid, F.; Roldan Cuenya, B. Nanoepitaxy Using Micellar Nanoparticles. *Nano Lett.* **2011**, *11*, 5290−5296.
(17) Diebold, U. the Surface Science of Titanium Dioxide. *Surf. Sci. Rep.* **2003**, *48*, 53−229.
(18) Wahlstrom, E.; Lopez, N.; Schaub, R.; Thostrup, P.; Ronnau, A.; Africh, C.; Laegsgaard, E.; Norskov, J. K.; Besenbacher, F. Bonding of Gold Nanoclusters to Oxygen Vacancies on Rutile TiO_2(110). *Phys. Rev. Lett.* **2003**, *90*.
(19) Park, J. B.; Conner, S. F.; Chen, D. A. Bimetallic Pt-Au Clusters on TiO_2(110): Growth, Surface Composition, and Metal-Support Interactions. *J. Phys. Chem. C* **2008**, *112*, 5490−5500.
(20) Behafarid, F.; Roldan Cuenya, B. Coarsening Phenomena of Metal Nanoparticles and the Influence of the Support Pre-Treatment: Pt/TiO_2(110). *Surf. Sci.* **2012**, DOI: 10.1016/j.susc.2012.01.022.
(21) Tauster, S. J.; Fung, S. C.; Garten, R. L. Strong Metal-Support Interactions - Group-8 Noble-Metals Supported on TiO_2. *J. Am. Chem. Soc.* **1978**, *100*, 170−175.
(22) Datye, A. K.; Kalakkad, D. S.; Yao, M. H.; Smith, D. J. Comparison of Metal-Support Interactions in Pt/TiO_2 and Pt/CeO_2. *J. Catal.* **1995**, *155*, 148−153.
(23) Pesty, F.; Steinruck, H. P.; Madey, T. E. Thermal-Stability of Pt Films on TiO_2(110) - Evidence for Encapsulation. *Surf. Sci.* **1995**, *339*, 83−95.
(24) Bonanni, S.; Ait-Mansour, K.; Brune, H.; Harbich, W. Overcoming the Strong Metal-Support Interaction State: CO Oxidation on TiO_2(110)-Supported Pt Nanoclusters. *ACS Catal.* **2011**, *1*, 385−389.
(25) Bowker, M.; Bennett, R. A. The Flexible Surface or the Rigid Surface? *Top. Catal.* **2001**, *14*, 85−94.
(26) Stone, P.; Smith, R. D.; Bowker, M. The Structure and Reactivity of Anchored Nanoparticles on a Reducible Support. *Faraday Discuss* **2004**, *125*, 379−390.
(27) Bennett, R. A.; Stone, P.; Bowker, M. Scanning Tunnelling Microscopy Studies of the Reactivity of The TiO_2(110) surface: Re-Oxidation and the Thermal Treatment of Metal Nanoparticles. *Faraday Discuss* **1999**, *114*, 267−277.
(28) Kim, M. H.; Baik, J. M.; Zhang, J. P.; Larson, C.; Li, Y. L.; Stucky, G. D.; Moskovits, M.; Wodtke, A. M. TiO_2 Nanowire Growth Driven by Phosphorus-Doped Nanocatalysis. *J. Phys. Chem. C* **2010**, *114*, 10697−10702.
(29) Lee, J. C.; Park, K. S.; Kim, T. G.; Choi, H. J.; Sung, Y. M. Controlled Growth of High-Quality TiO_2 Nanowires on Sapphire and Silica. *Nanotechnology* **2006**, *17*, 4317−4321.
(30) Berko, A.; Kiss, A. M.; Szoko, I. Formation of Vacancy Islands Tailored by Pt Nanocrystallites and Ar^+ Sputtering on TiO_2(110) Surface. *Appl. Surf. Sci.* **2005**, *246*, 174−182.
(31) Li, M.; Hebenstreit, W.; Diebold, U.; Tyryshkin, A. M.; Bowman, M. K.; Dunham, G. G.; Henderson, M. A. The Influence of the Bulk Reduction State on the Surface Structure and Morphology of Rutile TiO_2(110) Single Crystals. *J. Phys. Chem. B.* **2000**, *104*, 4944−4950.
(32) Bowker, M.; Bennett, R. A. The Role of Ti^{3+} Interstitials in TiO_2(110) Reduction and Oxidation. *J. Phys.: Condens. Matter* **2009**, 21.
(33) Henderson, M. A. A Surface Perspective on Self-Diffusion in Rutile TiO_2. *Surf. Sci.* **1999**, *419*, 174−187.
(34) Bowker, M.; Fourre, E. Direct Interactions between Metal Nanoparticles and Support: STM Studies of Pd on TiO_2(110). *Appl. Surf. Sci.* **2008**, *254*, 4225−4229.
(35) Iddir, H.; Ogut, S.; Zapol, P.; Browning, N. D. Diffusion Mechanisms of Native Point Defects in Rutile TiO_2: Ab Initio Total-Energy Calculations. *Phys. Rev. B* **2007**, 75.
(36) Hoshino, K.; Peterson, N. L.; Wiley, C. L. Diffusion and Point-Defects in TiO_{2-x}. *J. Phys. Chem. Solids* **1985**, *46*, 1397−1411.
(37) Mulheran, P. A.; Nolan, M.; Browne, C. S.; Basham, M.; Sanvillee, E.; Bennett, R. A. Surface and Interstitial Ti Diffusion at the Rutile TiO_2)(110) Surface. *Phys. Chem. Chem. Phys.* **2010**, *12*, 9763−9771.
(38) Jacobsen, J. Island Shapes in Homoepitaxial Growth of Pt(111). *Surf. Sci.* **1996**, *359*, 37−44.
(39) Cronemeyer, D. C. Electrical and Optical Properties of Rutile Single Crystals. *Phys. Rev.* **1952**, *87*, 876−886.
(40) Roldan Cuenya, B.; Croy, J. R.; Mostafa, S.; Behafarid, F.; Li, L.; Zhang, Z.; Yang, J. C.; Wang, Q.; Frenkel, A. I. Solving the Structure of Size-Selected Pt Nanocatalysts Synthesized by Inverse Micelle Encapsulation. *J. Am. Chem. Soc.* **2010**, *132*, 8747.
(41) Naitabdi, A.; Ono, L. K.; Behafarid, F.; Roldan Cuenya, B. Thermal Stability and Segregation Processes in Self-Assembled Size-Selected Au_xFe_{1-x} Nanoparticles Deposited on TiO_2(110): Composition Effects. *J. Phys. Chem. C* **2009**, *113*, 1433−1446.
(42) Paredis, K.; Ono, L. K.; Mostafa, S.; Li, L.; Zhang, Z. F.; Yang, J. C.; Barrio, L.; Frenkel, A. I.; Roldan Cuenya, B. Structure, Chemical Composition, and Reactivity Correlations during the in Situ Oxidation of 2-Propanol. *J. Am. Chem. Soc.* **2011**, *133*, 6728−6735.